



Cite this: *RSC Adv.*, 2024, **14**, 15441

## Calcium alginate elastic capsules for microalgal cultivation

Du Tuan Tran,<sup>a</sup> Nhat-Khuong Nguyen,<sup>1D a</sup> Ajeet Singh Yadav,<sup>a</sup> Ann Chuang,<sup>b</sup> Michele Burford,<sup>\*b</sup> Chin Hong Ooi,<sup>1D a</sup> Kamalalayam Rajan Sreejith<sup>a</sup> and Nam-Trung Nguyen <sup>1D \*</sup><sup>a</sup>

Calcium alginate elastic capsules with a core–shell structure are versatile spherical solid beads that can be produced in large quantities using various techniques. This type of capsule is a promising platform for cell culture applications, owing to its mechanical elasticity and transparency. This paper reports the production of calcium alginate capsules with high consistency, and for the first time, demonstrates the feasibility of the capsules for microalgal cultivation. Cell growth analysis reveals that the vibrationally-shaken calcium alginate elastic capsule platform yielded a higher maximum cell number ( $4.86 \times 10^8$  cells per mL) during the cultivation period than the control solution platforms. Aquafeed and food supplements for humans are the targeted applications of this novel platform.

Received 20th January 2024  
 Accepted 7th May 2024

DOI: 10.1039/d4ra00519h  
[rsc.li/rsc-advances](http://rsc.li/rsc-advances)

### 1. Introduction

Microalgae is a class of microscopic single-cell organisms that can convert carbon dioxide, solar energy, and inorganic nutrients into biomass and oxygen through the photosynthesis process. Compared to macroflora, microalgae have advantages such as higher biomass productivity, faster growth rate, and the ability to survive in a wide range of aquatic environments with a small amount of mineral nutrients. Hence, microalgae have been produced on a large scale to be used as food supplements, specialty cosmetic products, medicines, or as a feedstock for conversion into biofuels.<sup>1–4</sup> Recently, some studies suggested that microalgae can also be cultivated to harvest oxygen for applications such as space exploration and wound treatment.<sup>5–8</sup>

Artificial microalgae cultivation methods have been devised to produce microalgae on a large scale. Currently, open raceway ponds and closed photobioreactors (PBRs) are the two most common large-scale microalgal cultivation methods.<sup>9</sup> The earliest microalgae cultivation method is the open raceway pond method, in which microalgae are cultivated inside a wide-open, shallow artificial pond. The biggest advantage of this method is low operation costs, however, it faces an extremely sizeable challenge of cross-contamination which affects the final yield of microalgae.<sup>10</sup> Thus, PBRs are devised to create a strictly controlled and enclosed environment for growing microalgae with high yield. In PBRs, nutrients, and carbon dioxide are constantly supplied while the lighting period is

adjusted accordingly to different strains of microalgae to ensure effective microalgae production.<sup>11</sup> However, currently, large-scale cultivation of microalgae using PBRs is still limited, notably due to its high operation costs.<sup>12</sup>

Digital micro elastofluidic platforms are flexible micro-scale solid-like capsules containing liquid. These platforms can be either a liquid droplet encapsulated by a solid shell, or as a liquid containing bead made of a polymeric matrix. The shell or the polymeric matrix serve as a protective barrier, effectively minimising contamination that affect the function of encapsulated contents. In addition, the shell or the matrix can be engineered to become transparent and semi-permeable, allowing for light penetration, gas exchange, and diffusion of molecules.<sup>13–15</sup> As a result, these platforms represent favourable environments for the encapsulation and growth of diverse cell types, including microalgae. Recently, our team made a successful attempt in capturing and cultivating microalgal cells inside liquid marble – a typical digital micro elastofluidic platform with a porous shell made of micro/nanoparticles. By enwrapping microalgae-containing aqueous droplet with silica nanoparticles, we created a microscale photobioreactor with a transparent and porous outer layer, enabling 30-fold increase in cell density within 5 day cultivation period.<sup>16</sup> In addition, polymeric matrix such as hydrogel has been used for microalgal immobilisation and subsequent cultivation. Hydrogel beads can provide a stable environment for sustainable cell growth with efficient gas and nutrient exchange with the surrounding medium. In addition, the robust hydrogel three-dimensional matrices immobilise the microalgal cells within the beads during the cultivation period, minimising the risk of cell leakage into surrounding environments and facilitating the effective cell retrieval process after cultivation. For these

<sup>a</sup>Queensland Micro- and Nanotechnology Centre, Griffith University, 170 Kessels Road, Nathan 4111 Queensland, Australia. E-mail: nam-trung.nguyen@griffith.edu.au

<sup>b</sup>Australian Rivers Institute, Griffith University, 170 Kessels Road, Nathan 4111 Queensland, Australia



reasons, calcium alginate hydrogel beads have been investigated thoroughly for microalgal cell cultivation-related applications such as agricultural uses, biofuel, chemical production, food supplements, and wastewater treatment.<sup>17–20</sup> For instance, de Jesus *et al.* successfully utilized calcium alginate hydrogel beads containing immobilized *Desmodesmus subspicatus* microalgal strain for the removal of potassium, carbon, and nitrogen from sugarcane vinasse. Detailed analysis demonstrated the stability of the hydrogel beads throughout the cultivation experiments, leading to a significant removal of potassium, carbon, and nitrogen (up to 28%, 38%, and 27% respectively) due to microalgae metabolism.<sup>21</sup> In a separate study, Alfaro-Sayes developed a closed two-stage flask approach to immobilize and cultivate cyanobacterium *Synechocystis* sp. PCC 6803 within calcium alginate hydrogel beads, resulting in increased dry cell weight compared to the free-cell cultivation method. This enhanced growth effect was utilized for the continuous production of succinate, a versatile biochemical compound with numerous applications.<sup>22</sup>

While the cultivation methods involving hydrogel beads and, more recently, liquid marbles have demonstrated their efficacy, both platforms come with their respective drawbacks. For liquid marbles, due to the rapid evaporation rate of the liquid through the porous shell, a specialised setup is required to maintain the humidity and counteract excessive evaporation.<sup>16</sup> Meanwhile, for hydrogel beads, although the matrix provides support for three-dimensional proliferation of cells, the high crosslinking density of the matrix can potentially impose spatial restrictions and hinder microalgae to achieve their maximum growth potential.<sup>23,24</sup> Core–shell elastic capsule with transparent, semi-permeable and mechanically robust shell is a promising digital micro elastofluidic platform for microalgal cultivation. Elastic capsule can be submerged in aqueous media for extended periods, eliminating the need for a humidity-controlled environment. In addition, elastic capsule has a liquid core, providing more space for cells to thrive compared to hydrogel beads. These beneficial features for cell growth has long rendered elastic capsules valuable for applications in human cell culture.<sup>25–27</sup> For instance, Nebel *et al.* managed to encapsulate and grow mesenchymal stem cells (MSCs) inside alginate-based elastic capsules using simple inverse gelation for capsule formation. Proliferation measurement showed that the cell number increased 2.5 times after four days.<sup>28</sup>

In the present study, we attempted to cultivate microalgae inside core–shell elastic capsule. For making the shell, we opted for the use of sodium alginate, a biodegradable polymer known for its environmentally friendly nature and widespread accessibility. We employed the inverse gelation technique to generate the elastic capsules because of its gentle conditions and low processing costs. We selected *Chlorella vulgaris*, one of the most studied and widely used microalgal strains as the main subject to study microalgae growth inside calcium alginate capsules. *Chlorella vulgaris* is known for its exceptional resilience in harsh environments as well as its ability to produce high nutritional values.<sup>18,29–31</sup> The microalgae cultivation setup based on calcium alginate capsule has the potential to evolve into a commercial platform due to the ease of fabrication, low cost of raw materials

and minimal contamination. Extracted dry microalgae cells with a high nutritional value from capsules can be used as food for fish or food supplements for human consumption.

## 2 Materials and methods

Sodium alginate, calcium lactate, and carboxymethyl cellulose (CMC) were obtained from Sigma-Aldrich. *Chlorella vulgaris* microalgal strain, codename CS-41, was obtained from the Commonwealth Scientific and Industrial Research Organisation (CSIRO). BG-11 culture medium was obtained from the Australian Rivers Institute (ARI) at Griffith University, Australia. The chemicals, culture media, and other apparatus were UV-sterilized prior to experiments.

### 2.1. Experimental setup

**2.1.1. Fabrication of blank elastic capsule.** Liquid-filled calcium alginate elastic capsules were fabricated using the inverse gelation technique.<sup>32,33</sup> Calcium lactate was used as the calcium ion source for ionotropic gelation of sodium alginate polymer strands, whereas carboxymethyl cellulose was used as a thickener to stabilize the core droplet upon contact with the bath solution. First, 0.5 g of calcium lactate was added into 20 mL of Milli-Q water under gentle stirring (300 rpm). Next, 0.2 g of carboxymethyl cellulose powder was gradually added into the premixed calcium lactate solution under vigorous stirring (800 rpm), until a clear, transparent without any visible clumps was obtained, indicating the thorough homogeneity of the core solution. Subsequently, 1 mL of the homogeneous core solution was formed using a micropipette and extruded slowly into 20 mL of 1% sodium alginate bath under low stirring speed (300 rpm) to form calcium alginate elastic capsules with a core–shell structure. The distance between the tip of the micropipette and the surface of the sodium alginate bath was maintained at 3 cm at all times. The elastic capsules were then rinsed in water to get rid of excess sodium alginate, which might cause the capsules to adhere to each other. Finally, all the rinsed capsules were collected for further characterization, including formation consistency and geometrical analysis.

**2.1.2. Preparation of elastic capsule containing *Chlorella vulgaris* and two control solutions.** Prior to the generation of elastic capsules, a designated amount of *Chlorella vulgaris* stock culture was added into the core solution under vigorous stirring so that the volume-to-volume ratio between the stock culture and the core solution was 1 : 10. The starting concentration of microalgae in the core solution, and also in the resulting capsules is (5.75 × 10<sup>5</sup> cells per mL). Next, elastic capsules were created using the same process as described in Section 2.2.1. The resulting elastic capsules containing *Chlorella vulgaris* stock culture were rinsed with water to get rid of residual sodium alginate. The purpose of water rinsing for these capsules is the same with blank capsules.

**2.1.3. Cultivation of elastic capsule containing *Chlorella vulgaris* and two control solutions.** We prepared two 12-well culture plates that contained an identical number of calcium alginate elastic capsules and control solutions. For elastic



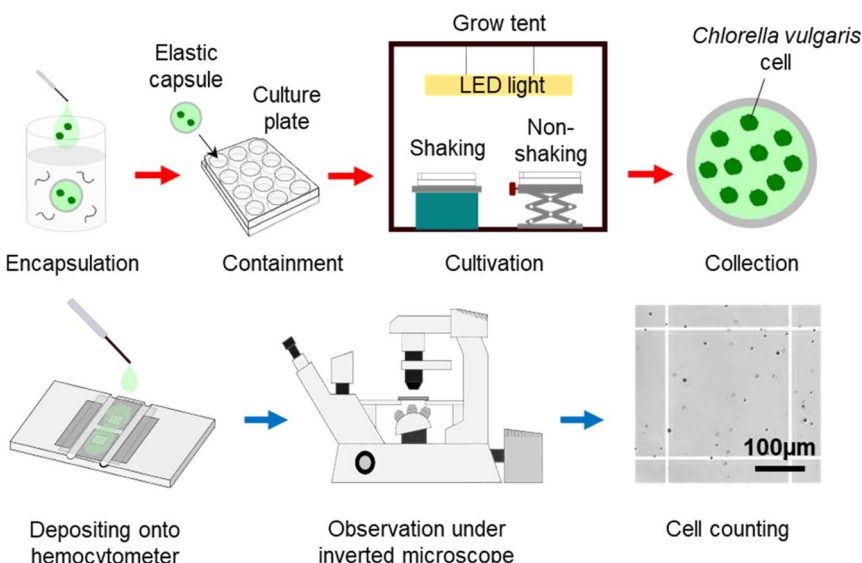


Fig. 1 Encapsulation, cultivation of *Chlorella vulgaris* in calcium alginate elastic capsules and cell counting procedure: (a) encapsulation and cultivation of *Chlorella vulgaris*; (b) cell counting of *Chlorella vulgaris*.

capsule culture, 60 capsules were separated evenly into wells of the culture plate, containing BG-11 medium of the same volume as control solutions. This process was repeated for another culture plate. One culture plate was placed on a vibrational shaker, while the other was placed on a vertical translation stage, as shown in Fig. 1a. The setups were placed in a growth tent, which served as a cultivation chamber. The height of the translation stage was adjusted to be the same as the surface of the shaker so that both culture plates could receive the same amount of light. The culture plate on the shaker was subjected to a shaking speed of 60 rpm. The artificial light needed for the photosynthesis of *Chlorella vulgaris* was provided by a LED grow light, which was set on a daily 12 hour light/12 hour dark cycle. The temperature of the cultivation chamber was maintained at  $25^{\circ}\text{C} \pm 1$  throughout the entire cultivation process. Cell counting was performed daily to investigate the growth behaviour of *Chlorella vulgaris* in the capsules and control solutions. The total cultivation time was 14 days.

## 2.2. Characterization

**2.2.1. Capsules geometrical characterization.** Photos of calcium alginate capsules were taken by a 1.3 MP Ximea Color CMOS Camera with USB 3.1 interface. A VZM™ 450 Zoom Imaging Lens by Edmund Optics was attached to the camera for better live inspection and imaging of the capsules. The captured photos were then analysed with ImageJ to determine the volume, size, and outer-to-inner diameter ratio of the capsules.

Sphericity factor calculation was adopted to determine the sphericity of the alginate capsules. The equation for the sphericity factor is as below:<sup>34–36</sup>

$$S = \frac{d_{\max} - d_{\min}}{d_{\max} + d_{\min}}, \quad (1)$$

where  $S$  is the sphericity factor,  $d_{\max}$  is the maximum diameter of the capsule and  $d_{\min}$  is the minimum diameter of the capsule.

**2.2.2. Measurement of LED growth light.** Growth light spectrum and photosynthetic photon flux density (PPFD) of grow light were measured using the MAVOSPEC BASE spectrometer. Fig. 2 shows the measured spectrum of the light. The spectrum indicates that the LED growth light has high red and blue intensity, which favours the growth of *Chlorella vulgaris*.<sup>37</sup> Furthermore, the measurement showed that the growth light has a PPFD of  $56 \pm 5 \mu\text{mol m}^{-2} \text{ s}^{-1}$ .

**2.2.3. Cell counting of control solutions.** To start with, a volume of  $10 \mu\text{L}$  of the solution was diluted with  $90 \mu\text{L}$  Milli-Q water. The diluted solution of control solution and Milli-Q water was agitated by a vortex mixer for 1 minute to ensure homogeneity. Next,  $10 \mu\text{L}$  of the diluted solution was extracted and injected into the Neubauer cell counting chamber, which was then placed under a Nikon Eclipse Ti2 Inverted Microscope for cell observation. Images of the cells were taken using the microscope. The photos were subsequently analysed using ImageJ (NIH, USA) for accurate cell counting and determination of final cell numbers.

**2.2.4. Cell counting of an elastic capsules.** First, the chosen calcium alginate capsule was submerged in  $400 \mu\text{L}$  of  $0.2 \text{ M}$

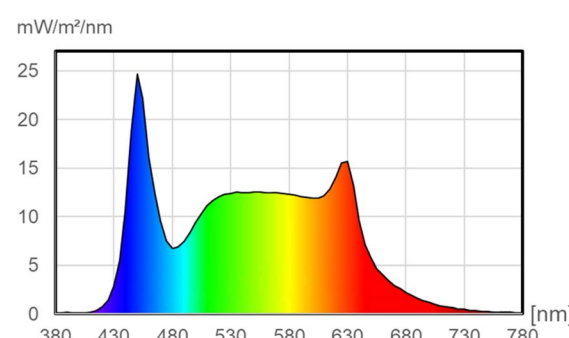


Fig. 2 The wavelength spectrum of LED growth light.



sodium citrate solution, which was then agitated vigorously by a vortex mixer for 2 minutes to facilitate the capsule dissolution process. Next, the cell counting process was carried out using the same method as described above for solutions.

Cell density (cells per mL) was calculated using the average cell number as the basis. The cell density equations for the solutions and the elastic capsules are determined as follow:

$$P = \frac{N \times D}{V_c} \quad (2)$$

where  $P$  is the cell density (cells per mL),  $N$  is the average cell number and  $D$  is the dilution factor. The dilution factor for solution is  $D = 10$ . The dilution factor for capsules is  $D = (400 + V_{\text{capsule}})/V_{\text{core}}$ , where  $V_{\text{capsule}}$  ( $\mu\text{L}$ ), is the total volume of capsule and  $V_{\text{core}}$  ( $\mu\text{L}$ ) is the volume of the core.  $V_c$  is the volume of the counting squares ( $1 \text{ mm}^2$  in area and  $0.1 \text{ mm}$  in depth) on the hemocytometer ( $V_c = 0.0001 \text{ mL}$ ).

**2.2.5. Specific growth rate and doubling time.** The specific growth rate is a constant that indicates the rate of increase of cell number per unit time in the exponential growth phase. The cell growth curve is required for the accurate calculation of specific growth rate. First, data on cell numbers over time was plotted in the form of a semi-log curve where the  $y$ -axis was displayed in a natural logarithmic scale. Next, the exponential growth phase was identified on the semi-log curve by determining the period where the cell number data points form a straight line with a positive slope. Finally, the specific growth rate was calculated using the slope of the straight line, which can be described below:

$$\mu = \frac{dP}{dt}, \quad (3)$$

where  $\mu$  is the specific growth rate (per day), and  $dP/dt$  is the rate of increase of cell number per unit time.

Doubling time refers to the time taken for microalgae to double in cell number. The doubling time is determined as:

$$t_d = \frac{\ln 2}{\mu}, \quad (4)$$

where  $t_d$  is the doubling time (day).

### 3. Results and discussion

#### 3.1. Consistency of elastic capsule formation process

In this study, the formation of calcium alginate elastic capsules and encapsulation of *Chlorella vulgaris* inside the capsules were carried out by manual extrusion using a micropipette. The volume of extrusion was fixed at 1 mL. The consistency of the capsule formation process was investigated by analysing two key factors: (i) the number of core solution droplets that came out from the micropipette and the number of elastic capsules successfully formed in the bath solution, and (ii) the geometrical parameters of the capsules.

Fig. 3 consolidates the results for consistency verification of elastic capsule formation. For comparison between the number of droplets and the number of capsules, the core solution was extruded 10 times into a 50 mL sodium alginate bath, each time

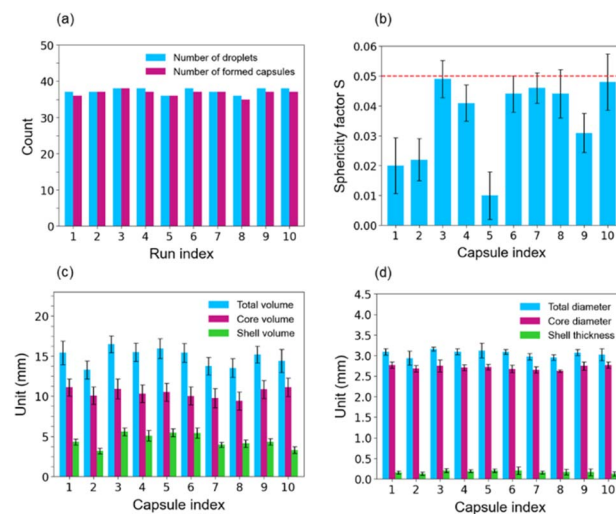


Fig. 3 Calcium alginate elastic capsule characterization: (a) comparison between the number of core solution droplets and number of formed capsules; (b) sphericity factor calculation; (c) comparison between total volume, core volume, and shell volume of capsules; (d) comparison between total diameter. Error bars represents standard deviation of three measurements.

1 mL. Fig. 3a indicates that almost all the core solution droplets generated from the micropipette were successfully enwrapped by calcium alginate hydrogel shell and subsequently turned into capsules in all the test runs, demonstrating the excellent consistency of the droplet formation method in this study.

In terms of shape, Fig. 4b shows that all elastic capsules have good spherical shapes since the sphericity factor of all of them was below 0.05.<sup>36</sup> Furthermore, the geometrical parameters of 10 randomly measured elastic capsules (Fig. 3c and d) show slight variations between the measured capsules. However, these variations are acceptable due to possible distortion of capsules caused by turbulence of bath solution during mixing. It also can be seen from these two figures that the calcium alginate capsules have a thin shell as proven by small shell

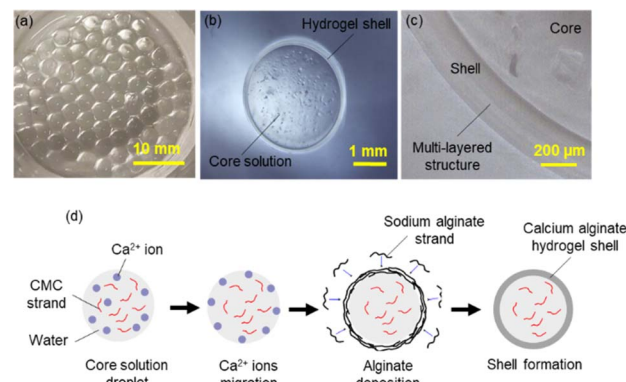


Fig. 4 Structure and formation of a calcium alginate elastic capsule: (a) elastic capsules after collection from alginate bath; (b) spherical elastic capsule with liquid core and hydrogel shell; (c) hydrogel shell with layer-by-layer structure; (d) hydrogel shell formation via layer-by-layer deposition onto core solution droplet.



volume (4.48  $\mu\text{L}$  in average) and low thickness (0.171 mm in average). That means that the core of each alginate capsule accounts for about 70% of total capsule volume, which is solely dedicated to encapsulation of the content. In addition, thin shell feature of capsules would facilitate the shell dissolution, allowing for more rapid extraction of contents inside the core for further treatments or analysis.

Fig. 4a and b shows blank spherical calcium alginate elastic capsules with core–shell structures. We can see that the capsule has high transparency, which allows the suspended contents in the core to be observed. Particularly, Fig. 4c shows the layer-by-layer structure of the hydrogel shell, which acts as a mechanically-stable physical barrier to protect the *Chlorella vulgaris* from external contamination. When a droplet of core solution meets the bath solution, sodium alginate molecules from the bath solution quickly deposit on the outer surface of the core solution and interact with calcium ions inside the droplet to form a hydrogel layer. Since calcium ions are still abundant after the formation of the first hydrogel layer, more sodium alginate molecules migrate to the liquid–solid interface of the first layer. This process is repeated until calcium ions are depleted. As a result, a robust layer-by-layer shell of the capsule was formed.<sup>38,39</sup> Fig. 4d illustrates the layer-by-layer deposition mechanism of sodium alginate onto the core solution droplet to form an elastic capsule.

### 3.2. Growth behaviour of *Chlorella vulgaris* inside calcium alginate elastic capsules

For comparison purposes, two other culture platforms were also prepared as control solutions: free culture and core solution-based free culture. The growth medium of the free culture was solely BG-11 solution, whereas the growth medium of the core solution-based free culture is a suspension that has the same initial chemical composition with core solution of an elastic capsule. The reason for the introduction of core solution-based free culture was to investigate the possible effect of calcium lactate and carboxymethylcellulose to microalgal growth under open environment without physical barrier such as capsule's shell. The volume-to-volume ratio between stock culture of *Chlorella vulgaris* and core solution or BG-11 was 1 : 10, the same as the ratio for elastic capsules. The initial cell numbers in capsules and free culture platforms are the same. In this way, capsule culture platforms and control platforms had the same starting microalgal concentration ( $5.75 \times 10^5$  cells per mL).

Fig. 5 shows images of calcium alginate capsules at different stages of cultivation. On the first day, *Chlorella vulgaris* cells were hardly observed on both platforms. The cells began to multiply rapidly from day 3 and filled up the entire core volume of both shaken and non-shaken capsules. From day 6, the effect of shaking started to take place on the capsules, proven by differences in cell distribution inside the core. For non-shaken capsules, microalgal cells accumulated at one side of the inner wall of the hydrogel shell, whereas in shaken capsules, the cells are dispersed evenly. This contrast of cell assembly was maintained until the end of the cultivation process, as shown by images captured on day 14.

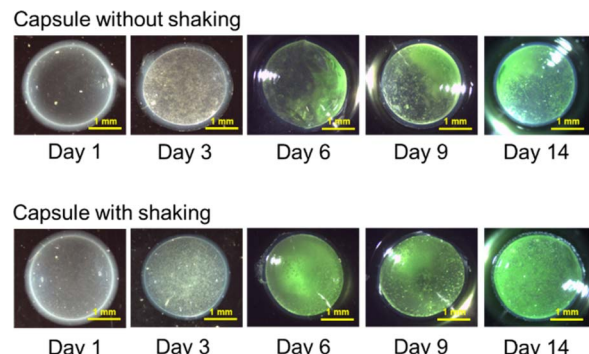


Fig. 5 Evolution of *Chlorella vulgaris* cells inside non-shaken and shaken elastic capsules.

Regarding structural stability, both non-shaken and shaken capsules preserved their overall shape without significant distortion. However, some minor deteriorations in the hydrogel shells were observed in both cases on day 6 and day 14, Fig. 5. This can be due to the calcium ion sequestration effect of some chelating agents presented in the BG-11 medium, causing a small portion of hydrogel to degrade. However, we observed that microalgal cells remained intact inside the core of shaken and non-shaken capsules without leaking out throughout the entire cultivation process.

### 3.3. Cell growth analysis of *Chlorella vulgaris*

In general, microalgae growth can be divided into four main phases: (i) lag phase, (ii) exponential phase, (iii) stationary phase, and (iv) death phase.<sup>38</sup> During the lag phase, microalgae are not actively dividing because they are adjusting themselves to the surrounding new environment. After this, microalgal cells divide and grow rapidly throughout the exponential phase, where specific growth rate and doubling time are commonly used to characterize the microalgae growth at this phase. The growth of microalgae begins to slow down with a minimal increase in cell number during the stationary phase, because of nutrient depletion, accumulation of toxic wastes, or increased competition for growth resources from other bacterial strains in the case of contamination. After an extended stationary period, the growth of microalgae progresses to the final death phase where the number of cells dying exceeds the number of cells being produced, leading to the eventual collapse of the culture and the cells. In this study, we stopped our cell counting measurement when all the growth curves reached the stationary phase, which is already sufficient for concluding the growth efficiency of the studied cell culture platforms.

Fig. 6a and b show cell number curves of control solutions and calcium alginate elastic capsules, respectively. The curves were plotted using individual data points that were collected daily using the cell counting process described in Sections 2.3.3 and 2.3.4. All cell culture platforms experienced a lag phase between day 1 and day 2, indicated by minor fluctuations in cell numbers. However, deviation of growth curves occurred in the exponential phase, where microalgal cells in the platforms behave differently from each other. Both control solution



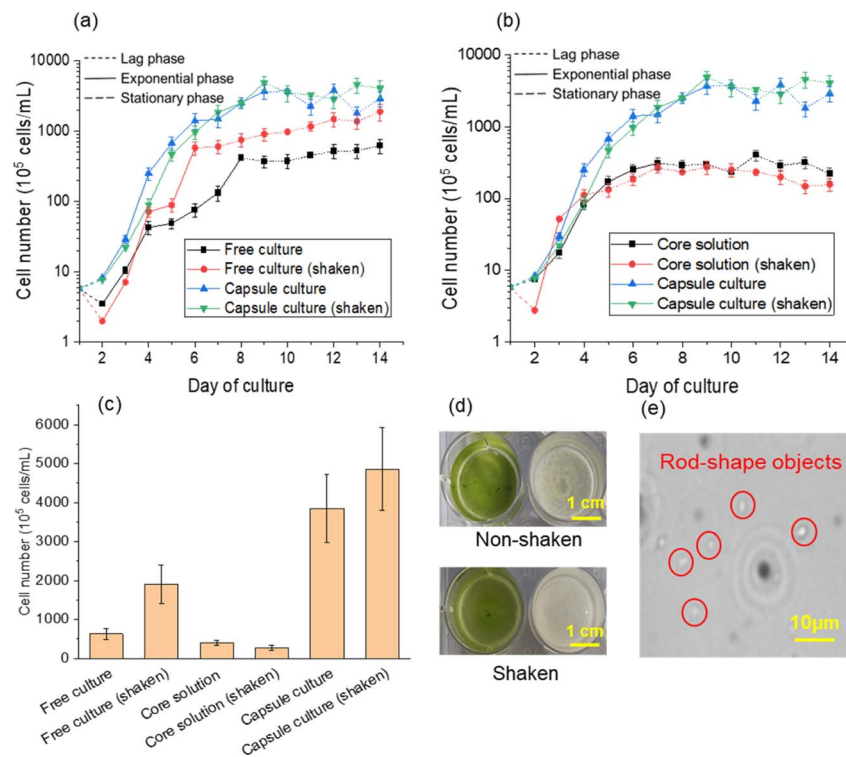


Fig. 6 Growth profile of *Chlorella vulgaris*: (a) cell number profile of capsule culture against free culture (shaken and non-shaken); (b) cell number profile of capsule culture against core solution-based free culture (shaken and non-shaken); (c) maximum cell numbers of free culture, core solution-based free culture and capsule culture (shaken and non-shaken); (d) difference in colours between free culture and core solution free culture (shaken and non-shaken); (e) microscopic photo of core solution free culture with rod-shape objects. The error bars represent the standard deviation of three measurements.

platforms, free cultures, and core solution free cultures exhibited shorter exponential growth phases than capsule counterparts. The exponential phase of capsule cultures lasted from day 2 to day 9 for both shaken and non-shaken platforms, whereas the exponential phase of control solutions ended on day 4, 7, or 8. We hypothesize that due to the absence of a physical barrier in both control solution platforms, microalgae cells can freely access the surrounding nutrients and thus divide faster. Meanwhile, in a capsule culture, the presence of the hydrogel shell of capsules might have a negative influence on the degree of access to nutrient molecules in the medium and microalgae inside the core of capsules, resulting in a lower metabolism rate of microalgal cells.

Regarding the maximum cell number observed during the 14 day cultivation period, capsule culture platforms performed better than both control solutions as depicted in Fig. 6c. The counted cell number ( $4.86 \times 10^8$  cells per mL) of shaken capsule culture is the highest among all the culture platforms. Excess nutrients from the surrounding medium might be a possible explanation for the more productive cell division of *Chlorella vulgaris* inside the capsules. Although the starting cell numbers were the same, the actual initial cell weight inside the core of a capsule was significantly less than in the control solutions due to the substantial difference in volume ( $\sim 16 \mu\text{L}$  of capsule *versus* 3 mL of control solution). Hence, capsule culture platforms exhibited a higher nutrient-to-cell mass ratio as compared to

control solution platforms, and therefore microalgal cells in the capsules had more available nutrients to grow sustainably.

The core solution free culture platforms exhibited lower maximum cell numbers compared with the other two platforms. This can be attributed to the culture crash caused by the possible gradual precipitation of calcium carbonate of core solution platforms. Calcium carbonate is likely formed *via* a biomineralization process called Microbially-induced Calcium Carbonate Precipitation (MICP), where carbonate ions produced from the metabolism activities of microalgal cells and calcium ions in the environment combine.<sup>39-41</sup> Fig. 6d reveals that both shaken and non-shaken core solution-based free culture platforms had white-yellow colour instead of green like the free culture ones, implying the existence of calcium carbonate which is a white powder. This assumption is further strengthened by the presence of rod-shape objects as shown in Fig. 6e, which are likely the calcium carbonate powder clumps. It is likely that these clumps were separated from microalgal cells due to the effect of agitation when preparing diluted solution for cell counting. Meanwhile, free culture platforms and capsule culture platforms were not affected by this issue. Free culture solution did not contain calcium lactate, whereas the capsules were washed thoroughly with water before cultivation to get rid of excess calcium ions from the cores.

Fig. 7 shows the rates of microalgal cell growth, and the times required for a cell number to double. All shaken



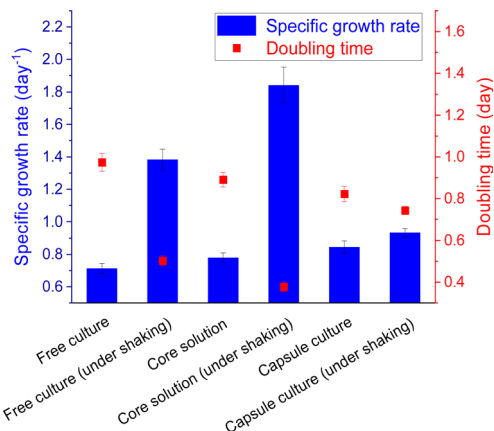


Fig. 7 Specific growth rates and doubling times of control solution platforms and capsule platforms. The error bars represent the standard deviation of three measurements.

platforms possessed higher specific growth rates and shorter doubling times. This result signifies the positive effect of vibrational shaking on the growth efficiency of microalgal cells. However, the discrepancy in specific growth rates and doubling times of shaken and non-shaken capsule culture platforms was not as significant as the one of the control solutions. Compared with freely floated microalgal cells in control solution platforms, cells in capsules had poorer mobility due to space constraints. Therefore, the effect of shaking on cell growth efficiency was reduced. This result also agrees well with the extended exponential phase of both capsule platforms as mentioned earlier.

## 4. Conclusion

This paper reports the development of a novel, easy-to-produce cell culture platform based on calcium alginate elastic capsules for microalgae *Chlorella vulgaris*. Despite the manual capsule generation method, geometrical characterizations demonstrated the uniform size, volume, and shell thickness of the generated capsules. For the evaluation of cultivation efficiency, we compared the growth parameters of microalgal cells inside the capsules with two control solution platforms. The results showed that both shaken and non-shaken capsule culture platforms reached higher maximum cell numbers than the controls, up to  $4.6 \times 10^8$  cells per mL (for shaken capsules). In addition, by rinsing thoroughly with water to remove residual calcium ions, the capsule culture eventually did not suffer from calcium carbonate precipitation issues, which might adversely affect the cell growth. However, long exponential phases accompanied by relatively low specific growth rates are the drawbacks that need to be addressed in future works. In terms of application, the capsules containing *Chlorella vulgaris* cells can be collected for post-cultivation treatments to harvest the dry microalgal biomass, which can be used as food sources for fish or humans. Investigation into possible direct oral consumption of elastic capsules after cultivation would be another potential research direction. Chemical components of

capsules, including calcium lactate, carboxymethylcellulose sodium alginate/calcium alginate, and encapsulated microalgae used in this study are edible.<sup>42–45</sup> Hence, the cultivated capsule-microalgae platform can possibly be directly consumed without the need to extract the microalgal biomass, if future studies prove that residual BG-11 solution on the capsules can be removed conveniently.

## Conflicts of interest

There are no conflicts to declare.

## Acknowledgements

N. T. N. acknowledge the support from the Australian Research Council (ARC) Discovery Project (Grant No. DP220100261). This work was partly performed at the Queensland node at Griffith University of the Australian National Fabrication Facility, a company established under the National Collaborative Research Infrastructure Strategy to provide nano and micro-fabrication facilities for Australian researchers.

## References

- 1 R. Sathasivam, R. Radhakrishnan, A. Hashem and E. F. Abd Allah, *Saudi J. Biol. Sci.*, 2019, **26**, 709–722.
- 2 M. Rizwan, G. Mujtaba, S. A. Memon, K. Lee and N. Rashid, *Renewable Sustainable Energy Rev.*, 2018, **92**, 394–404.
- 3 S. Y. A. Siddiki, M. Mofijur, P. S. Kumar, S. F. Ahmed, A. Inayat, F. Kusumo, I. A. Badruddin, T. M. Y. Khan, L. D. Nghiem, H. C. Ong and T. M. I. Mahlia, *Fuel*, 2022, **307**.
- 4 Y. Maltsev and K. Maltseva, *Rev. Environ. Sci. Bio/Technol.*, 2021, **20**, 515–547.
- 5 S. P. Miguel, M. P. Ribeiro, A. Otero and P. Coutinho, *Algal Res.*, 2021, **58**, 102395.
- 6 R. Corrales-Orovio, F. Carvajal, C. Holmes, M. Miranda, S. Gonzalez-Itier, C. Cardenas, C. Vera, T. L. Schenck and J. T. Egana, *Acta Biomater.*, 2023, **155**, 154–166.
- 7 M. L. Obaid, J. P. Camacho, M. Brenet, R. Corrales-Orovio, F. Carvajal, X. Martorell, C. Werner, V. Simon, J. Varas, W. Calderon, C. D. Guzman, M. R. Bono, S. San Martin, A. Eblen-Zajjur and J. T. Egana, *Front. Med.*, 2021, **8**, 772324.
- 8 E. D. Revellame, R. Aguda, A. Chistoserdov, D. L. Fortela, R. A. Hernandez and M. E. Zappi, *Algal Res.*, 2021, **55**, 102258.
- 9 G. Singh and S. K. Patidar, *J. Environ. Manage.*, 2018, **217**, 499–508.
- 10 J. Mehar, A. Shekh, N. M. U, R. Sarada, V. S. Chauhan and S. Mudliar, *J. CO<sub>2</sub> Util.*, 2019, **33**, 384–393.
- 11 P. Altimari, F. Di Caprio, A. Brasileiro and F. Pagnanelli, *Chem. Eng. Sci.*, 2023, **272**, 118604.
- 12 E. G. Nwoba, D. A. Parlevliet, D. W. Laird, K. Alameh and N. R. Moheimani, *Algal Res.*, 2019, **39**, 101731.
- 13 P. Singha, N. K. Nguyen, K. R. Sreejith, H. An, N. T. Nguyen and C. H. Ooi, *Adv. Mater. Interfaces*, 2020, **8**, 2001591.



14 L. Gorgannezhad, K. R. Sreejith, M. Christie, J. Jin, C. H. Ooi, M. Katouli, H. Stratton and N. T. Nguyen, *Micromachines*, 2020, **11**, 761–771.

15 D. T. Tran, A. S. Yadav, N. K. Nguyen, P. Singha, C. H. Ooi and N. T. Nguyen, *Small*, 2023, e2303435, DOI: [10.1002/smll.202303435](https://doi.org/10.1002/smll.202303435).

16 N.-K. Nguyen, D. T. Tran, A. Chuang, P. Singha, G. Kijanka, M. Burford, C. H. Ooi and N.-T. Nguyen, *React. Chem. Eng.*, 2023, **8**, 2710–2716.

17 D. Rajmohan and D. Bellmer, *Int. J. Food Sci.*, 2019, **2019**, 7101279.

18 G. Mujtaba and K. Lee, *Water Res.*, 2017, **120**, 174–184.

19 D. A. Alfaro-Sayes, J. Amoah, N. Rachmadona, S. Hama, T. Hasunuma, A. Kondo and C. Ogino, *J. Phys.: Energy*, 2023, **5**, 014019.

20 L. E. Gonzalez and Y. Bashan, *Appl. Environ. Microbiol.*, 2000, **66**, 1527–1531.

21 G. C. de Jesus, R. Gaspar Bastos and M. Altenhofen da Silva, *Biocatal. Agric. Biotechnol.*, 2019, **22**, 101438.

22 D. A. Alfaro-Sayes, J. Amoah, S. Aikawa, M. Matsuda, T. Hasunuma, A. Kondo and C. Ogino, *Biochem. Eng. J.*, 2022, **188**, 108681.

23 M. Han, C. Zhang and S. H. Ho, *Environ. Sci. Ecotechnology*, 2023, **14**, 100227.

24 W. P. Voo, P. Ravindra, B. T. Tey and E. S. Chan, *J. Biosci. Bioeng.*, 2011, **111**, 294–299.

25 F. M. Galogahi, Y. Zhu, H. An and N.-T. Nguyen, *J. Sci.: Adv. Mater. Devices*, 2020, **5**, 417–435.

26 W. Rao, S. Zhao, J. Yu, X. Lu, D. L. Zynger and X. He, *Biomaterials*, 2014, **35**, 7762–7773.

27 W. Bouhlel, J. Kui, J. Bibette and N. Bremond, *ACS Biomater. Sci. Eng.*, 2022, **8**, 2700–2708.

28 S. Nebel, M. Lux, S. Kuth, F. Bider, W. Dietrich, D. Egger, A. R. Boccaccini and C. Kasper, *BioEngineering*, 2022, **9**, 66–80.

29 M. T. Ahmad, M. Shariff, F. Md. Yusoff, Y. M. Goh and S. Banerjee, *Rev. Aquacult.*, 2018, **12**, 328–346.

30 C. Safi, B. Zebib, O. Merah, P.-Y. Pontalier and C. Vaca-Garcia, *Renewable Sustainable Energy Rev.*, 2014, **35**, 265–278.

31 H. Amini, L. Wang and A. Shahbazi, *Chem. Eng. Sci.*, 2016, **152**, 403–412.

32 A. H. Morales, F. C. Spuches, J. S. Hero, A. F. Alanís, M. A. Martínez and C. M. Romero, *Food Hydrocolloids*, 2021, **117**, 106706.

33 P. Russo, R. Zacco, D. M. Rekkas, S. Politis, E. Garofalo, P. Del Gaudio and R. P. Aquino, *J. Drug Delivery Sci. Technol.*, 2019, **49**, 577–585.

34 B. Balanc, A. Kalusevic, I. Drvenica, M. T. Coelho, V. Djordjevic, V. D. Alves, I. Sousa, M. Moldao-Martins, V. Rakic, V. Nedovic and B. Bugarski, *J. Food Sci.*, 2016, **81**, E65–E75.

35 J. Zhao, Q. Guo, W. Huang, T. Zhang, J. Wang, Y. Zhang, L. Huang and Y. Tang, *Polymers*, 2020, **12**, 688–903.

36 E. S. Chan, B. B. Lee, P. Ravindra and D. Poncelet, *J. Colloid Interface Sci.*, 2009, **338**, 63–72.

37 M. N. Metsoviti, G. Papapolymerou, I. T. Karapanagiotidis and N. Katsoulas, *Plants*, 2019, **9**, 31–47.

38 L. Zhu, *Biofuels, Bioprod. Biorefin.*, 2015, **9**, 801–814.

39 Z. W. Chin, K. Arumugam, S. E. Ashari, F. W. Faizal Wong, J. S. Tan, A. B. Ariff and M. S. Mohamed, *Molecules*, 2020, **25**.

40 K. Arumugam, R. Mohamad, S. E. Ashari, J. S. Tan and M. S. Mohamed, *Asia-Pac. J. Chem. Eng.*, 2022, **17**, e2767.

41 M. J. Castro-Alonso, L. E. Montañez-Hernandez, M. A. Sanchez-Muñoz, M. R. Macias Franco, R. Narayanasamy and N. Balagurusamy, *Frontiers in Materials*, 2019, **6**, 126.

42 F. Javaheri-Ghezeldizaj, J. Soleymani, S. Kashanian, J. Ezzati Nazhad Dolatabadi and P. Dehghan, *Microchem. J.*, 2020, 154.

43 L. Dou, B. Li, K. Zhang, X. Chu and H. Hou, *Int. J. Biol. Macromol.*, 2018, **118**, 1377–1383.

44 Y. Biao, C. Yuxuan, T. Qi, Y. Ziqi, Z. Yourong, D. J. McClements and C. Chongjiang, *Food Hydrocolloids*, 2019, **97**, 105197.

45 S. Li, Y. Ma, T. Ji, D. E. Sameen, S. Ahmed, W. Qin, J. Dai, S. Li and Y. Liu, *Carbohydr. Polym.*, 2020, **248**, 116805.

